

# Chemical Control of Hydrodynamic Instabilities in Partially Miscible Two-Layer Systems

M. A. Budroni,<sup>\*,†,§</sup> L. A. Riolfo,<sup>†</sup> L. Lemaigre,<sup>†</sup> F. Rossi,<sup>‡</sup> M. Rustici,<sup>¶</sup> and A. De Wit<sup>†</sup>

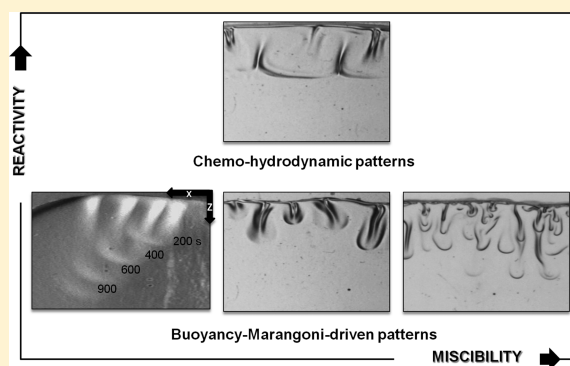
<sup>†</sup>Nonlinear Physical Chemistry Unit, Service de Chimie Physique et Biologie Théorique, Faculté des Sciences, Université libre de Bruxelles (ULB), CP231, 1050 Brussels, Belgium

<sup>‡</sup>Department of Chemistry and Biology, University of Salerno, via Giovanni Paolo II 132, 84084 Fisciano, Salerno, Italy

<sup>¶</sup>Department of Chemistry and Pharmacy, University of Sassari, Via Vienna 2, Sassari 07100, Italy

**ABSTRACT:** Hydrodynamic instabilities at the interface between two partially miscible liquids impact numerous applications, including CO<sub>2</sub> sequestration in saline aquifers. We introduce here a new laboratory-scale model system on which buoyancy- and Marangoni-driven convective instabilities of such partially miscible two-layer systems can easily be studied. This system consists of the stratification of a pure alkyl formate on top of a denser aqueous solution in the gravitational field. A rich spectrum of convective dynamics is obtained upon partial dissolution of the ester into the water followed by its hydrolysis. The properties of the convective patterns are controlled by the miscibility of the ester in water, the feedback of the dissolved species on its own miscibility, as well as the reactivity of given chemicals in the aqueous solution with the solubilized ester.

**SECTION:** Liquids; Chemical and Dynamical Processes in Solution



The study of buoyancy-driven convective mixing of partially miscible fluids has recently gained renewed interest because this process is at the heart of CO<sub>2</sub> sequestration techniques, in which supercritical CO<sub>2</sub> is injected into underground aquifers or petroleum reservoirs. After injection, the CO<sub>2</sub> rises up to the impermeable cap rock, forming a layer of less dense liquid on top of the denser brine or alkanes in which it partially dissolves. The denser layer of dissolved CO<sub>2</sub> then starts to sink into the lower liquid because of a buoyancy-driven instability favoring further dissolution and mixing.<sup>1,2</sup> Chemical reactions can affect this dissolution because of their feedback on the miscibility of CO<sub>2</sub> and on the density gradients<sup>3,4</sup> and hence on the buoyancy-driven mixing. Reaction products may also influence surface tension gradients at the partially miscible interface and thus trigger Marangoni flows. Such phenomena are difficult to explore in situ, and simple model systems on which fundamental experimental studies can be performed are needed.

Investigations of such interfacial hydrodynamic instabilities have up to now been mainly focused on either fully miscible or totally immiscible two-layer systems. In miscible systems, Rayleigh–Taylor and double-diffusive instabilities have long been known to affect stratification of nonreactive fluids in the gravity field.<sup>5</sup> For reactive systems, convective dynamics have also been experimentally and theoretically studied,<sup>6</sup> showing how the reaction can severely change the symmetry of convective modes.<sup>7</sup> Nonreactive double-layer miscible systems with nonideal mixing properties have also been proposed to mimic supercritical CO<sub>2</sub> dynamics at the interface with

aquifers.<sup>8,9</sup> However, the studies of such miscible interfaces can only address buoyancy-driven convection and cannot take into account the influence of partial miscibility and surface tension effects on convective instabilities and transport phenomena.

In parallel, in immiscible two-layer systems, coupling of reactions with buoyancy- and Marangoni-driven instabilities is responsible for a variety of patterns and complex spatiotemporal dynamics including oscillations and interfacial turbulence.<sup>10–14</sup> Typically, these systems consist of two layers of immiscible fluids in which the diffusion-controlled transfer of one or more solutes diffusing from one solvent to the other provides the engine for chemical processes as well as density and surface tension gradients at the origin of convective motions.<sup>15</sup> Convection can develop in both phases, and chemo-hydrodynamic processes are eventually dominated by a diffusion-limited regime.<sup>16</sup> Immiscible systems lack thus the specificity of partially miscible systems, which is a constant feeding of reaction–diffusion–convection (RDC) dynamics thanks to the one-way-directed transfer of matter from the infinite reservoir of one pure liquid phase toward the “host” one, governed by a solubilization process. In that case, buoyancy- and Marangoni-driven convective motions can maintain a strong feedback with the mass transfer rate.<sup>17</sup> When a chemical reaction impacts the solubilization kinetics,

Received: January 8, 2014

Accepted: February 7, 2014

the chemical environment and physics of the system also change in time, further affecting the stability between the two layers.<sup>18,19</sup> Despite the interest for CO<sub>2</sub> sequestration and other applications,<sup>20,21</sup> studies and classification of RDC dynamics around spatially extended partially miscible interfaces are however missing.

In this Letter, we introduce the partially miscible stratification of an ester on top of a denser aqueous solution reactor as a rich laboratory-scale model system for experimental and theoretical studies of chemo-hydrodynamic instabilities at the interface between two partially miscible liquids. We also demonstrate how chemical reactions in the aqueous phase allow for a direct control of the hydrodynamic instabilities. This system features all specific characteristics of spatiotemporal convective dynamics in partially miscible systems and of their dependence on the miscibility, the solubilization kinetics, and chemical transformations.

Alkyl formates are organic ester compounds of general formula HCOOR', where R' is an alkyl chain. They are partially miscible in water with a solubilization constant  $\chi_e = e_o/e_{(\text{org})}$ , where  $e_o$  and  $e_{(\text{org})}$  represent the dimensional concentration of the alkyl formate in the saturated water phase and the dimensional pure ester concentration in the organic phase, respectively (see Table 1 and ref 22). In water, alkyl formates

**Table 1. Values of the Experimental Parameters for Three Alkyl Formates, HCOOR', with Increasing Alkyl Chain<sup>a</sup>**

alkyl chain (R')	$\rho_e$ at 20 °C (g cm <sup>-3</sup> )	$(1/\rho_w)(\partial\rho/\partial e)$ (M <sup>-1</sup> )	$\chi_e^{22}$ (%)
methyl- (-CH <sub>3</sub> )	0.974	0.0060 ± 0.0005	30
ethyl- (-CH <sub>2</sub> CH <sub>3</sub> )	0.921	0.0020 ± 0.0010	10
propyl- (-CH <sub>2</sub> CH <sub>2</sub> CH <sub>3</sub> )	0.904	na	0.2

<sup>a</sup> $\rho_w = 0.9982$  g cm<sup>-3</sup> is the pure water density at 20 °C.

undergo a slow spontaneous hydrolysis in neutral conditions to produce formic acid, HCOOH, and the alcohol, R'OH. The kinetics of the hydrolysis process is autocatalytic in acidic conditions<sup>23</sup> and is also considerably accelerated in an alkaline environment.<sup>24</sup> In aqueous solutions of alkaline hydroxides (MOH), the ester reacts with the base to yield a formate salt (HCOOM) and an alcohol (R'OH), according to the scheme



where M stands for the metal counterion of OH<sup>-</sup>. We study the chemo-hydrodynamic properties of the ester/water system in a quasi-two-dimensional geometry, where the less dense pure ester phase is set on top of the denser aqueous layer in the gravity field. The experimental setup consists of a Hele-Shaw cell made of two borosilicate glass plates separated by a thin polymer mask giving a gap width of 1 mm.<sup>25</sup> The dynamics in the colorless solutions is followed by an optical phase-shifting Schlieren technique<sup>26,27</sup> visualizing the variations in space and time of the refractive index, which are related to the density gradients inside of the solutions. All experimental images have a field of view of 2 cm × 2 cm. Reagent-grade reactants (Sigma-Aldrich) are used without further purification.

The typical convective instability observed with a short alkyl chain formate (methyl formate) is shown in Figure 1a. Starting from a buoyantly stable configuration, a hydrodynamic density

fingering instability develops below the interface upon dissolution of pure methyl formate in the denser pure water. Here, the hydrolysis process is extremely slow with respect to the time scale at which the hydrodynamic instability occurs, and convective motions are induced by the local accumulation of the dissolved ester, HCOOCH<sub>3(aq)</sub>, just below the contact line between the aqueous and the organic phases. The convective dynamics is localized in the aqueous layer. Convective flows further enhance the solubilization of the ester in the water phase, thus feeding the instability similarly to what is observed in convective dissolution of CO<sub>2</sub> in water.<sup>1</sup> Once the fingers appear, they grow along the gravitational field, but they also exhibit a slow horizontal drift from the center to the borders of the cell (and vice versa), forming preferential hydrodynamic paths where fingers merge and persist in time (see also Figure 1c). As the formate dissolves into the water, the interface not only tends to move upward, it also ripples and exhibits the formation of soliton-like horizontal waves, reminiscent of dissipative waves observed at the surface of liquids in Marangoni-driven flows.<sup>28,29</sup> The presence of an interfacial Marangoni contribution to the flow can be attributed here to the ester transfer into water and to the slow production of the alcohol that, even in traces, can induce strong surface activity.<sup>15</sup> In order to check the relative weight in the convective flows of vertical buoyancy-driven motions versus horizontal Marangoni flows close to the interface, we performed analogous experiments with the cell perpendicularly oriented with respect to the gravitational field. With this horizontal configuration, no convective motions could be detected, indicating that, contrarily to the buoyancy-induced flows, Marangoni-driven convection is not suitable by itself to initiate the solubilization process and, thus, can be considered as a side effect also in the phenomenology of vertical experiments carried out in neutral conditions.

When the top layer is ethyl formate or propyl formate, buoyancy-driven fingering is also observed (Figure 1b,c). As for the methyl formate, convective dissolution is here dominated by the solubilization process rather than by the hydrolysis reaction. Comparing Figure 1a–c, we see that the system is less unstable when the length of the alkyl chain R' increases as less fingers appear and as they grow on a longer time scale. In the case of propyl formate/water, we observe just one finger emerging over a time scale 2 orders of magnitude slower with respect to the methyl formate/water stratification. In the space–time plot of Figure 1c (right panel), we can appreciate the convective dynamics in which the fingers travel horizontally along the contact line, with a speed comparable to the slow vertical development. The instability growth rate follows the tendency of these esters to mix in water as convection develops more vigorously for shorter alkyl formates that are more miscible in water. However, it is opposite to the reactivity that, according to kinetic investigations,<sup>23</sup> increases with the alkyl chain length.

The relative importance of the miscibility and of the reactivity of the ester in the convective dissolution dynamics can be rationalized by means of a minimal model in which the solubilization and reactive processes are coupled with the Stokes equations, governing the evolution of the velocity field  $\mathbf{v} = (u, v)^T$  in the reactor. We consider a two-dimensional vertical slab in a reference frame  $(x, z)$ , in which the gravitational vector  $\mathbf{g}$  is oriented against the vertical direction  $z$ . Because the upper organic phase is not affected by the hydrodynamic flows, we focus our description on the bottom aqueous layer of width  $L_x$

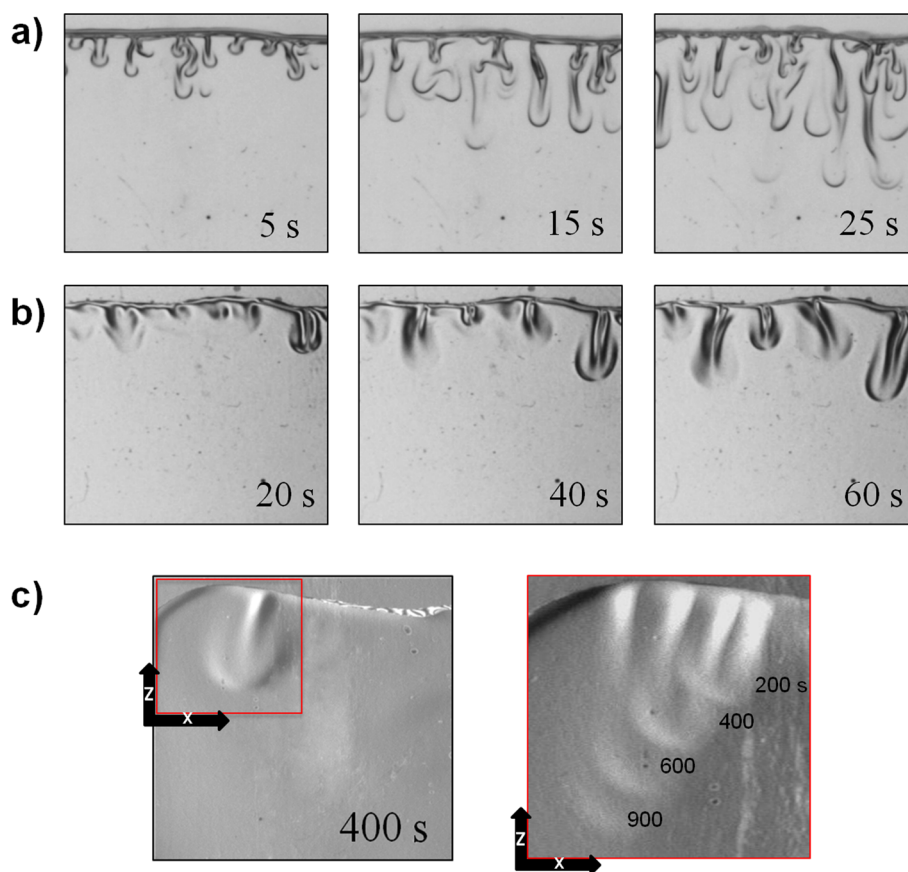


**Figure 1.** Typical density fingering observed experimentally below the horizontal interface between pure water and pure methyl formate (a), ethyl formate, (b) and propyl formate (c). The ester lies on top of the aqueous phase. In (c), the space–time plot in the right panel follows at successive times the vertical growth and the horizontal drifting of the finger shown in the left panel within the red frame of size  $0.95 \text{ cm} \times 0.95$ .

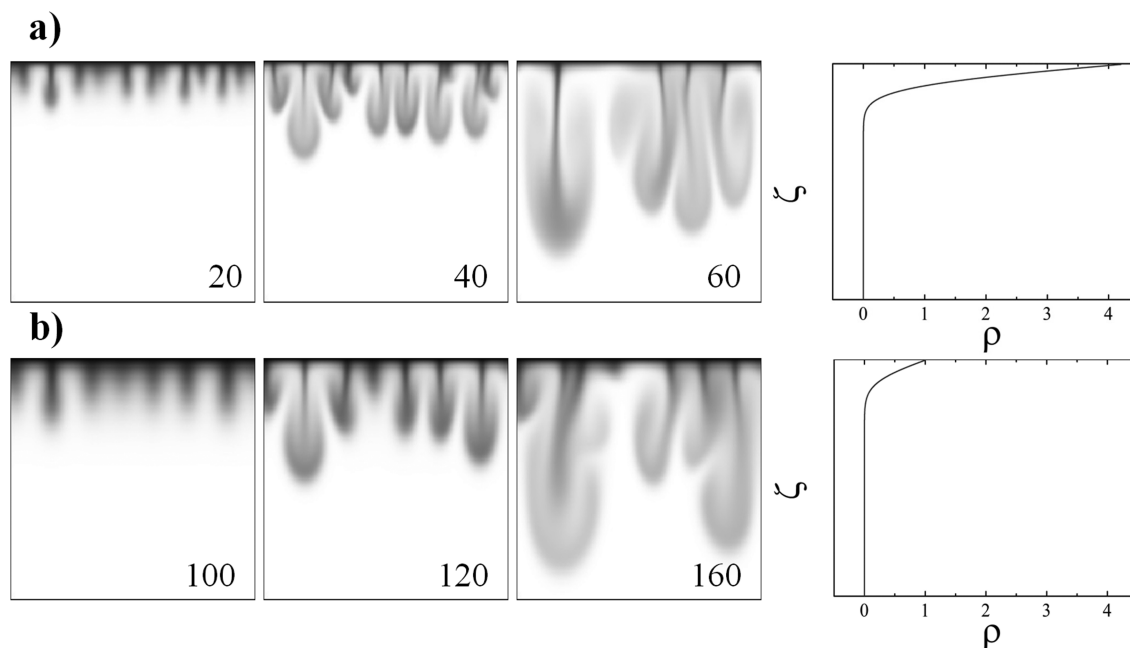


**Figure 2.** Spatiotemporal dynamics of the ester concentration computed numerically for the nonreactive convective dissolution of methyl formate/water (a) and ethyl formate/water (b) stratification. The last snapshot of each row shows the asymptotic dimensionless density profile ( $R_e = 1$ ), which has a self-similar form in the rescaled variable  $\zeta = z/(D_e t)^{1/2}$ . To emphasize the difference in the density profile of the two systems, concentration values are scaled over the ethyl formate concentration in the saturated water phase. The spatial domain of numerical simulations is  $400 \times 400$  space units.

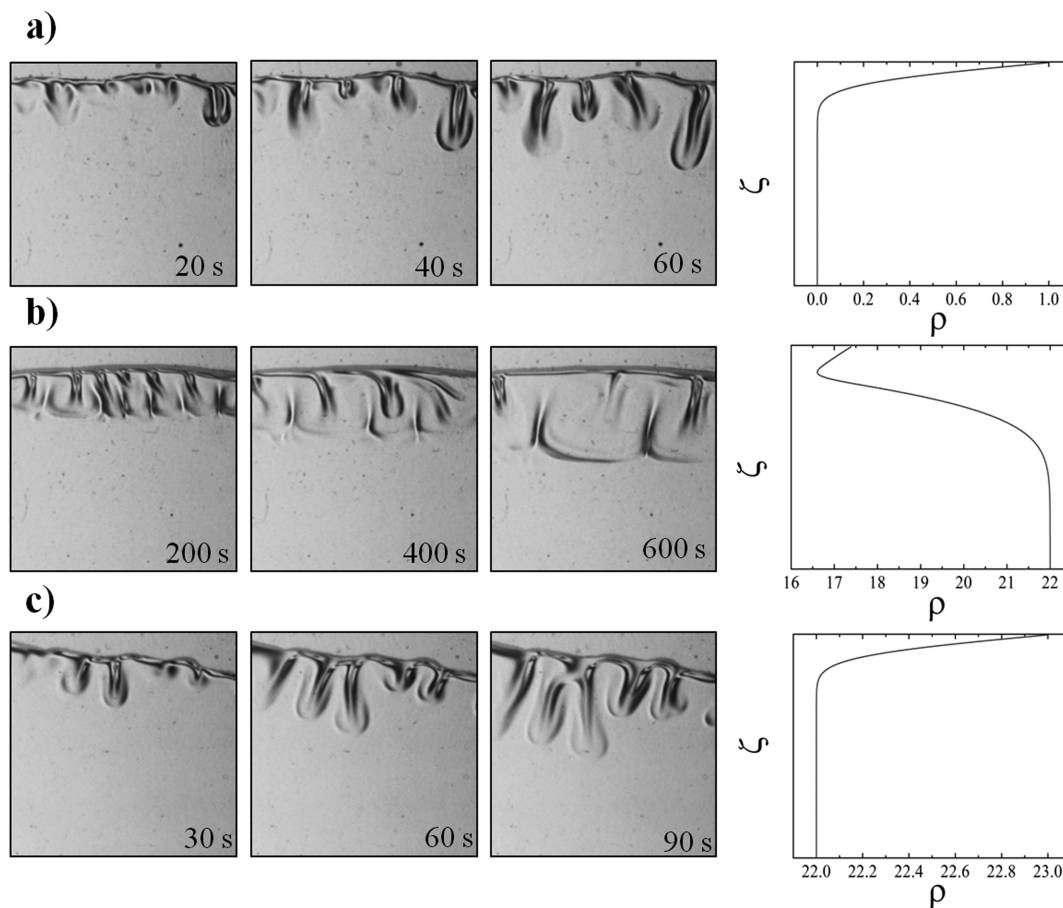


**Figure 3.** Experimental spatiotemporal dynamics below of the interface between ethyl formate and (a) pure water, (b) 1 M NaOH solution, and (c) 1.07 M NaCl solution. In the (b) and (c), the aqueous solutions have the same initial density. The last snapshot of each row shows the asymptotic density profile computed numerically, as described in the text by using  $R_{\text{HCOOEt}} = 1.0$ ,  $R_{\text{NaOH}} \approx 22.0$ ,  $R_{\text{HCOONa}} = 20.5$ , and  $R_{\text{EtOH}} = -4.1$ .

and height  $L_z$ . Moreover, as the upward drifting of the interface is negligible on the hydrodynamic time scale, the reference frame is kept fixed. No-slip boundary conditions are imposed to the velocity field, and no-flux at all boundaries are used for all concentrations except at the top where we take a constant value  $e_o$  boundary condition for the ester. This mimics the constant amount of formate solubilizing at the interface from the upper phase, which, under the hypothesis of local equilibrium, is given by the solubility  $e_o = e_{L_z} = \chi_e e_{(\text{org})}$ .<sup>30</sup> The dimensionless RDC equations<sup>6,32</sup> are written in the Boussinesq approximation and in the vorticity-stream function ( $\omega - \psi$ ) form

$$\frac{\partial c_i}{\partial t} + \left( \frac{\partial \psi}{\partial z} \frac{\partial c_i}{\partial x} - \frac{\partial \psi}{\partial x} \frac{\partial c_i}{\partial z} \right) = \delta_i \nabla^2 c_i + \mathcal{D}f_i$$

$\forall$   $i$ th chemical species (2)

$$\nabla^2 \omega = \sum_i R_i \frac{\partial c_i}{\partial x}$$
(3)

$$\frac{\partial^2 \psi}{\partial x^2} + \frac{\partial^2 \psi}{\partial z^2} = -\omega$$
(4)

where the horizontal and the vertical components of the velocity field are tied to the stream function through the relations  $u = \partial_z \psi$  and  $v = -\partial_x \psi$ . The  $c_i$  indicates the dimensionless aqueous concentration of the  $i$ th species, and  $f_i$  is the related chemical kinetics. In our description, we introduce

the Damköhler number  $\mathcal{D}$  as the ratio between the hydrodynamic and the chemical time scales.<sup>32</sup> In neutral conditions, the reactive process can be neglected with respect to the hydrodynamic characteristic time scale (thus,  $\mathcal{D} \rightarrow 0$ ), and the aqueous alkyl formate with dimensionless concentration  $c_e$  is the only species ruling the system instability. The second-order kinetics  $f_i = kc_e c_{\text{MOH}}$  describing reaction 1 comes into play when we consider the alkaline hydrolysis. In this case, the hydrodynamic and the chemical time scales are comparable ( $\mathcal{D} \approx 1$ ), and the reaction products are also taken into account in the model along with the ester and the base. For simplicity, the diffusivity ratios  $\delta_i = D_i/D_e$  between each species diffusivity  $D_i$  and the ester diffusivity in water  $D_e$  are all taken equal to unity. The buoyancy ratio  $R_i = (\partial \rho / \partial [i]) / (\partial \rho / \partial e)$  quantifies the relative contribution of the  $i$ th species to the local dimensionless density as

$$\rho(i) = \sum_i R_i c_i$$
(5)

As shown in Figure 2, the main dynamical features observed experimentally for the different alkyl formates are well-reproduced numerically and can be understood in terms of the dimensionless asymptotic density profiles.<sup>6,7</sup> These are derived by introducing in eq 5 the numerical asymptotic concentration profiles of the pure reaction–diffusion problem (eq 2) (with  $\psi = 0$ ) and the proper values for the buoyancy ratio  $R_i$  of each active chemical species as given in Figure 2. At

long times ( $t \rightarrow \infty$ ), the reaction–diffusion solutions converge to a self-similar concentration profile in the rescaled variable  $\zeta = z/(D_e t)^{1/2}$ . In the nonreactive case, the density profiles in the aqueous layer (see the last snapshots in Figure 2) show a local maximum at the top of the water phase where the dissolving alkyl formate produces a mass accumulation with respect to the bottom region. The density jump decreases as the alkyl chain length becomes longer, that is, when the decrease in solubility leads to a smaller density maximum. As supported by the numerical simulations in Figure 2, the effect is that the less soluble ester (Figure 2b) produces a smaller density jump below the interface and hence slow-growing fingers while the instability readily develops with the more soluble methyl formate (Figure 2a). Both experimental and numerical evidence lead us to propose the solubilization constant of an ester,  $\chi_e$ , as the main parameter influencing the density jump at the interface in nonreactive conditions and, hence, the onset time and the strength of the convective instability. In the modeling, this dependence on  $\chi_e$  (and on  $e_{(\text{org})}$ ) explicitly appears in the characteristic hydrodynamic time and spatial scales  $t_h$  and  $L_h$ .<sup>32</sup>

Control of the convective instabilities in this ester/water two-layer system can be achieved by tuning the density profile (i) by changing ad hoc the density profile of the aqueous solution (through local changes in temperature for instance<sup>33</sup>), (ii) by influencing ad hoc the ester solubilization through a suitable change of the chemical or physical environment in the aqueous layer (via the addition of an inert compound, for instance, or a change of the global temperature), and/or (iii) promoting in situ changes of type (i) and (ii) through a chemical reaction.

To demonstrate experimentally the efficiency of the scenario where chemistry strongly modifies the hydrodynamic instability, we analyze spatiotemporal dynamics of a reactive case when the hydrolysis process is catalyzed by a base, as in reaction 1. Solutions of NaOH are used in the lower layer, and the concentration of the alkaline solute is varied in the range if [0.01, 2.00] M. Figure 3 compares the nonreactive solubilization of ethyl formate in pure water (Figure 3a) with the reactive one in NaOH (Figure 3b). We observe, thanks to the reaction, a strong stabilization of fingering that develops at the same vertical extent as that in Figure 3a but on a much longer time scale. This is related to the fact that the solutal expansion coefficient of the sodium formate produced by the hydrolysis reaction (its contribution to the density has been measured to be  $(1/\rho_w)/(\partial\rho/\partial[\text{HCOONa}]) = 0.0410 \pm 0.0005 \text{ M}^{-1}$ ) is smaller than that of the base ( $(1/\rho_w)/(\partial\rho/\partial[\text{NaOH}]) = 0.044 \text{ M}^{-1}$ ; see ref 34). The formation upon reaction of alcohol also decreases the local density of the medium ( $(1/\rho_w)/(\partial\rho/\partial[\text{EtOH}]) = 0.0081 \text{ M}^{-1}$ ; see ref 34). The result is that if the initial amount of base is large enough to transform a significant part of aqueous alkyl formate into the related less dense salt and the alcohol, a nonmonotonic density distribution with a depletion zone below the interface develops along the gravity field (see the last snapshot in Figure 3b). This density minimum features a stabilizing barrier that refrains from the fingering growth. Note that relative changes in density as small as  $10^{-3}$  are already sufficient to trigger macroscopic convective motions in a few seconds.<sup>6,7</sup> Depending upon the relative contribution of the reactants and products to the total density, the fingering arising from a solubilization mechanism can thus be controlled by a reaction. In the case of a nonmonotonic density profile with a minimum like that in the case discussed above, convective patterns are prevented from developing downward. On the contrary, convective dissolution can be

enhanced if the density profile remains monotonic and the density maximum at the interface is intensified by the chemical process.

In Figure 4a, the stabilizing effect experienced in the alkaline hydrolysis is quantified as a function of the concentration of the

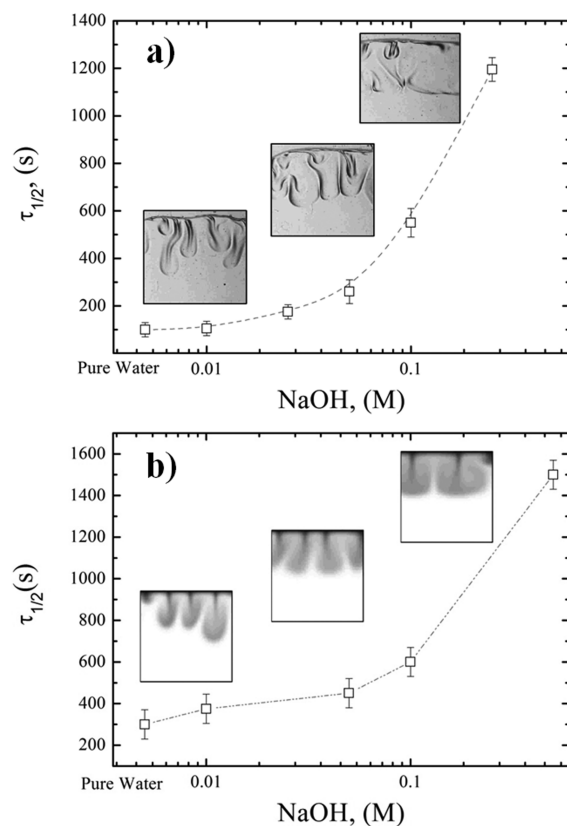


**Figure 4.** Experimental (a) and numerical (b) characteristic time  $\tau_{1/2}$  of the fingers growth as a function of the alkaline concentration of the aqueous phase.

base by computing  $\tau_{1/2}$ , the time required for the fingers to reach the mid length of the aqueous layer. This observable embeds average information on the fingering growth rate. The  $\tau_{1/2}$  values reported for each concentration point are averaged over six experiments, and the typical patterns obtained are also shown. There is an initial concentration domain where the dynamics is unaffected by the alkaline hydrolysis. For concentrations larger than  $[\text{NaOH}] = 0.1 \text{ M}$ , the system undergoes an increase in  $\tau_{1/2}$ . The slowing down of the instability goes along with a change in the finger's shape, which turns into "fatter" structures due to the dynamical formation of a minimum in the density profile (Figure 3b). The width of the fingers becomes larger as the alkaline solute concentration is increased and, typically, squared cells developing for  $[\text{NaOH}]$  larger than 1 M merge into a homogeneous stratification. It is worth remarking here that the control of the instability is completely governed by solutal density changes due to the reaction. Thermal contributions are negligible<sup>35</sup> while the shift of the aqueous solution density toward larger values is not able to induce the same effect on the finger growth and/or analogous patterns as a minimum in density. This can be verified by comparing the snapshots of Figure 3b and c, which show isopycnic aqueous phases but feature an alkaline and a neutral environment, respectively. When the inert salt NaCl is

added (Figure 3c), regular fingers with a faster characteristic time scale and a morphology comparable to those of the pure water case develop. This is because the density profile (even if shifted toward larger values by a constant due to the addition of NaCl) remains monotonically decreasing, that is, does not have the stabilizing minimum induced by the reaction with a base. The slight delay in the formation of the fingers with NaCl (Figure 3c) with regard to the neutral case (Figure 3a) might be due to an influence of NaCl on the solubility of the ester in the water, but this has not been quantified here. The trend and the patterns obtained by numerical integration of eqs 2–4, with the second-order kinetics of reaction 1, show a good qualitative and quantitative agreement with the experimental results (see Figure 4b). In particular, numerical simulations support the idea that even if the alkaline conditions speed up the formation of the alcohol that acts as a strong surfactant, buoyancy effects dominate the convective dynamics observed in the experiments.

To summarize, the dissolution of alkyl formates in a two-layer superposition of an ester on top of partially miscible denser water in the gravitational field is proposed as a model system to study hydrodynamic instabilities of the interface between two partially miscible fluids. Buoyancy-driven fingering occurs, driven by the solubilization process of the ester into the water layer. The degree of solubility of the ester in the water is a key parameter controlling the onset time and the intensity of the convective dissolution instability in nonreactive conditions, while the influence of the hydrolysis of the ester in the water has a secondary effect in neutral conditions. Changing the chemical composition of the aqueous solution allows one to achieve a chemical control on the instability by tuning the density profile in the water phase. As an example, a chemical reaction of the ester with an alkaline hydroxide in the aqueous solution can induce a depletion zone below the interfacial region thanks to the in situ formation of a less dense salt. The result is that the density profile becomes nonmonotonic, and the finger growth is refrained from or even substituted by a stable stratification. New chemo-hydrodynamic scenarios could be induced by the nonlinear interplay between chemical kinetics and more complicated solubilization mechanisms (see, for instance, ref 31). This work shows, among others, that an understanding of the impact of chemical reactions on convective dissolution and trapping processes, which are important in applied problems as complex as CO<sub>2</sub> sequestration, is a prerequisite to assess the optimal transport and dissolution conditions in partially miscible systems.

## AUTHOR INFORMATION

### Corresponding Author

\*E-mail: mabudroni@uniss.it

### Present Address

§M.A.B.: Department of Chemistry and Pharmacy, University of Sassari, Via Vienna 2, Sassari 07100, Italy.

### Notes

The authors declare no competing financial interest.

## ACKNOWLEDGMENTS

We acknowledge financial support from Prodex (M.A.B., L.L., and A.D.), ARC CONVINCERE (A.D.), FNRS FORECAST (A.D.), Regione Sardegna POR project (M.A.B. and M.R.), the ITN-Marie Curie-Multiflow network (L.A.R. and A.D.), and FRIA (L.L.).

## REFERENCES

- (1) Kneafsey, T. J.; Pruess, K. Laboratory Flow Experiments for Visualizing Carbon Dioxide-Induced Density-Driven Brine Convection. *Transp. Porous Media* **2010**, *3*, 123–139.
- (2) Kneafsey, T. J.; Pruess, K. Laboratory Experiments and Numerical Simulation Studies of Convectively Enhanced Carbon Dioxide Dissolution. *Energy Procedia* **2011**, *4*, 5114–5121.
- (3) Ennis-King, J.; Paterson, L. Coupling of Geochemical Reactions and Convective Mixing in the Long-Term Geological Storage of Carbon Dioxide. *Int. J. Greenhouse Gas Control* **2007**, *1*, 86–93.
- (4) Andres, J. T. H.; Cardoso, S. S. S. Onset of Convection in a Porous Medium in the Presence of Chemical Reaction. *Phys. Rev. E* **2011**, *83*, 046312.
- (5) Carballido-Landeira, J.; Trevelyan, P. M. J.; Almarcha, C.; De Wit, A. Mixed-Mode Instability of a Miscible Interface Due to Coupling Between Rayleigh–Taylor and Double-Diffusive Convective Modes. *Phys. Fluids* **2013**, *25*, 024107.
- (6) Almarcha, C.; Trevelyan, P. M. J.; Grosfils, P.; De Wit, A. Chemically Driven Hydrodynamic Instabilities. *Phys. Rev. Lett.* **2010**, *104*, 044501.
- (7) Lemaigre, L.; Budroni, M. A.; Riolfo, L. A.; Grosfils, P.; De Wit, A. Asymmetric Rayleigh–Taylor and Double-Diffusive Fingers in Reactive Systems. *Phys. Fluids* **2013**, *25*, 014103.
- (8) Backhaus, S.; Turitsyn, K.; Ecke, R. E. Convective Instability and Mass Transport of Diffusion Layers in a Hele–Shaw Geometry. *Phys. Rev. Lett.* **2011**, *106*, 104501.
- (9) Neufeld, J. A.; Hesse, M. A.; Riaz, A.; Hallworth, M. A.; Tchepeli, H. A.; Huppert, H. E. Convective Dissolution of Carbon Dioxide in Saline Aquifers. *Geophys. Res. Lett.* **2010**, *37*, L22404.
- (10) Sherwood, T. S.; Wei, J. C. Interfacial Phenomena in Liquid Extraction. *Ind. Eng. Chem.* **1957**, *49*, 1030–1034.
- (11) Eckert, K.; Grahn, A. Plumes and Finger Regimes Driven by an Exothermic Interfacial Reaction. *Phys. Rev. Lett.* **1999**, *82*, 4436–4439.
- (12) Eckert, K.; Acker, M.; Shi, Y. Chemical Pattern Formation Driven by a Neutralization Reaction. Part I: Mechanism and Basic Features. *Phys. Fluids* **2004**, *16*, 385–399.
- (13) Shi, Y.; Eckert, K. Orientation-Dependent Hydrodynamic Instabilities from Chemo-Marangoni Cells to Large Scale Interfacial Deformations. *Chin. J. Chem. Eng.* **2007**, *15*, 748–753.
- (14) Eckert, K.; Acker, M.; Tadmouri, R.; Pimienta, V. Chemo-Marangoni Convection Driven by an Interfacial Reaction: Pattern Formation and Kinetics. *Chaos* **2012**, *22*, 037112.
- (15) Sternling, C. V.; Scriven, L. E. Interfacial Turbulence: Hydrodynamic Instability and the Marangoni Effect. *AIChE J.* **1959**, *4*, 514–523.
- (16) Lavabre, D.; Pradines, V.; Micheau, J.-C.; Pimienta, V. Periodic Marangoni Instability in Surfactant (CTAB) Liquid/Liquid Mass Transfer. *J. Phys. Chem. B* **2005**, *109*, 7582–7586.
- (17) Mendes-Tassis, M. A.; Perez de Ortiz, E. S. Spontaneous Interfacial Convection in Liquid–Liquid Binary Systems Under Microgravity. *Proc. R. Soc. London* **1992**, *438*, 389–396.
- (18) Perez de Ortiz, E. S.; Sawistowski, H. Interfacial Stability of Binary Liquid–Liquid Systems-II. Stability Behavior of Selected Systems. *Chem. Eng. Sci.* **1973**, *28*, 2063–2069.
- (19) Agble, D.; Mendes-Tassis, M. A. The Effect of Surfactants on Interfacial Mass Transfer in Binary Liquid–Liquid Systems. *Int. J. Heat Mass Transfer* **2000**, *43*, 1025–1034.
- (20) Citri, O.; Kagan, M. L.; Kosloff, R.; Avnir, D. The Evolution of Chemically Induced Unstable Density Gradients Near Horizontal Reactive Interfaces. *Langmuir* **1990**, *6*, 559–564.
- (21) Savino, R.; Lappa, M. Dissolution and Solutal Convection in Partially Miscible Liquid Systems. *Int. J. Heat Mass Transfer* **2004**, *47*, 601–612.
- (22) Góral, M.; Shaw, D. G.; Maczyński, A.; Wiśniewska-Gocłowska, B.; Jezierski, A. IUPAC–NIST Solubility Data Series. 88. Esters with Water-Revised and Updated. Part 1. C<sub>2</sub> to C<sub>4</sub> Esters. *J. Phys. Chem. Ref. Data* **2009**, *38*, 1093–1127.
- (23) Jogunola, O.; Salmi, T.; Eranen, K.; Warna, J.; Kangas, M.; Mikkola, J. P. Reversible Autocatalytic Hydrolysis of Alkyl Formate:

Kinetic and Reactor Modeling. *Ind. Eng. Chem. Res.* **2010**, *49*, 4099–4106.

(24) Patai, S. *The Chemistry of Carboxylic Acids and Esters*; John Wiley and Sons Ltd: Chichester, New York, Brisbane, Toronto, 1969.

(25) Shi, Y.; Eckert, K. A Novel Hele–Shaw Cell Design for the Analysis of Hydrodynamic Instabilities in Liquid–Liquid Systems. *Chem. Eng. Sci.* **2008**, *63*, 3560–3563.

(26) Settles, G. S. *Schlieren and Shadowgraph Techniques*; Springer: Berlin, Heidelberg, Germany; New York, 2001.

(27) Joannes, L.; Dubois, F.; Legros, J.-C. Phase-Shifting Schlieren: High-Resolution Quantitative Schlieren that Uses the Phase-Shifting Technique principle. *Appl. Opt.* **2003**, *42*, 5046–5053.

(28) Weidman, P. D.; Linde, H.; Velarde, M. G. Evidence for Solitary Wave Behavior in Marangoni–Bénard Convection. *Phys. Fluids A* **1992**, *4*, 921–926.

(29) Schwarzenberger, K.; Köllner, T.; Linde, H.; Odenbach, S.; Boeck, T.; Eckert, K. On the Transition from Cellular to Wavelike Patterns during Solutal Marangoni Convection. *Eur. Phys. J.: Spec. Top.* **2013**, *219*, 121–130.

(30) These values are calculated as  $e_o = \chi_e e_{(org)}$ , where  $e_{(org)} = 15$  M for the methyl formate and 12 M for the ethyl formate. If needed, the boundary condition could involve a functional dependence of  $\chi_e$  on the concentration of the chemical species in order to describe the dynamical feedback of the reaction on the solubility of the ester in the water (see ref 31).

(31) Roque, C.; Pimienta, V.; Lavabre, D.; Micheau, J. C. Solubilization Processes in Autocatalytic Biphasic Reactions. *Langmuir* **2000**, *16*, 6492–6496.

(32) The concentrations, velocity field, spatial domain, and time are nondimensionalized by  $e_o$ ,  $u_h = gK\alpha_e e_o/\nu$ ,  $l_h = D_e/u_h$ , and  $t_h = D_e/u_h^2$ , respectively, where  $\alpha_e = (1/\rho_w)(\partial\rho/\partial e)$  is the solutal expansion coefficient of the solubilized ester,  $g$  is the magnitude of the gravitational acceleration,  $\nu$  and  $\rho_w$  are the kinematic viscosity and the density of water, respectively, and  $D_e$  is the diffusivity of the alkyl formate in the aqueous medium ( $\sim 10^{-8}$  cm<sup>2</sup> s<sup>-1</sup>).  $K$  is the permeability, equal to  $a^2/12$  for a Hele–Shaw cell with a gap width of  $a$ . The pressure scale is defined as  $p_a + \rho_w g z + \mu D_e/K$ , where  $p_a$  denotes the ambient pressure and  $\mu = \nu\rho_w$  is the water dynamic viscosity. The Damköhler number is defined as  $\mathcal{D} = t_h k e_o$ , where  $k$  is the kinetic constant of the ester hydrolysis and  $1/(k e_o)$  defines the chemical time scale.

(33) Bratsun, D. A.; Shi, Y.; Eckert, K.; De Wit, A. Control of Chemo-Hydrodynamic Pattern Formation by External Localized Cooling. *Europhys. Lett.* **2005**, *69*, 746–752.

(34) *CRC Handbook of Chemistry and Physics*, 56th ed.; CRC Press: Cleveland, OH; 1975–1976.

(35) Almarcha, C.; Trevelyan, P. M. J.; Grosfils, P.; De Wit, A. Thermal Effects on the Diffusive Layer Convection Instability of an Exothermic Acid–Base Reaction Front. *Phys. Rev. E* **2013**, *88*, 033009.